High-energy cluster—surface collisions

ARTICLE *in* CHEMICAL PHYSICS LETTERS · JANUARY 1993

Impact Factor: 1.9 · DOI: 10.1016/0009-2614(93)85282-S

3 AUTHORS, INCLUDING:

Uzi Even
Tel Aviv University
176 PUBLICATIONS **5,347** CITATIONS

SEE PROFILE

Joshua Jortner
Tel Aviv University
719 PUBLICATIONS **30,392** CITATIONS

SEE PROFILE

High-energy cluster–surface collisions

Uzi Even, Israel Schek and Joshua Jortner
School of Chemistry, Tel-Aviv University, Ramat Aviv, 69978 Tel-Aviv, Israel

Received 7 September 1992; in final form 3 November 1992

Molecular dynamics simulations of high-energy collisions (initial kinetic energies $E_k^0 = 10$–10^6 eV) of Kr_n ($n = 8$–512) clusters with a rigid Pt surface provide a microscopic description of the formation of an intracluster shock wave (temperatures up to 3×10^5 K and cluster internal potential energies up to $\sim10^4$ eV) on a time scale of 10–500 fs, which is accompanied by novel ultrafast energy acquisition processes. High-energy ($(10$–$5)\times10^3$ eV) high-yield (0.5%–10%) interatomic Kr–Kr pair repulsive excitation is exhibited, being manifested in outer-shell electronic excitations and ionization, multiple ionization and Auger processes.

Clusters allow for the exploration of the evolution of macroscopic surface and condensed matter properties [1,2]. Of considerable interest are dynamic cluster size effects [3,4], which fall into two categories:

(a) Intracluster dynamics [5–9]. These involve a variety of reactive and nonreactive processes, e.g., direct dissociation and evaporation, vibrational predissociation, vibrational energy redistribution and electronic–vibrational radiationless transitions.

(b) Cluster collisions. These involve cluster–cluster collisions, which exhibit fragmentation in molecular clusters [10], cluster fusion, deep elastic and quasi-elastic collisions in metal clusters [11], dissociative absorption of molecules on metal clusters [12], and isomerization reactions in ion–rare-gas clusters [13]. Another interesting class of collisional processes pertain to cluster–wall collisions [14–25].

Collisions of molecular clusters at moderate energies (up to 0.5 eV/atom) with surfaces exhibit dissociative cluster dynamics, which were rationalized in terms of multiple binary atom–atom collisions within the cluster in conjunction with atom–surface collisions [15,16]. The impact of high-energy large clusters (which was accomplished by the acceleration of cluster ions at typical velocities of up to 5×10^6 cm s^{-1} and energies of up to 500 keV) on solid surfaces [17–25] is of considerable interest for the following reasons:

(1) High-energy cluster–surface collisions are expected to produce high transient particle and energy densities [20,21]. Approximate model calculations [20] for the impact of deuterium clusters on metallic surfaces predict cluster compression up to ≈4 times the standard density at cluster velocities (prior to impact) of $v=6\times10^6$ cm s^{-1}.

(2) A microscopic shock wave is expected to be generated within the colliding cluster being manifested by large pressures and high temperatures, which are expected to be generated on a time scale of $\tau\sim R/v$, where R is the cluster radius [20,21]. Approximate estimates [20] for the impact of deuterium clusters on metallic surfaces at $v=6\times10^6$ cm s^{-1} predict pressures of 7 Mbars and temperatures of 10^5 K.

(3) High-energy cluster–surface collisions are expected to result in a multitude of novel energy storage and disposal phenomena, e.g., cluster fragmentation [15,16], outer-shell electronic excitation ionization and Auger core excitation [22,23] of fragments.

(4) Technological applications are of interest. A potential application may involve cluster-impact fusion [26–32] of $(D_2O)_n^+$ ($n=25$–1000) clusters at energies of 300 keV on deuterated surfaces [27,28], which is still not demonstrated experimentally [32], in accord with negative results from molecular dynamics (MD) simulations [29,30]. Applications of high-energy cluster–surface collisions in the area of material science involve controlled film growth [24],

surface modification, and microdrilling [21]. Utilization in the field of mass spectrometry involves sputtering of large biomolecules by massive cluster impacts [25].

When internally cold but rapidly moving clusters collide with a solid surface, a new medium, which constitutes a microscopic intracluster shock wave, is temporarily formed on the time scale of $\tau = 20$–500 fs [20–24]. In this letter, we have utilized classical MD simulations to explore the energy acquisition processes in high-energy cluster collisions with rigid metal surfaces, which will provide guidelines for (i) the characterization of a microscopic shock wave within the cluster; (ii) the energy disposal within the cluster during the collision; (iii) the time scale for energy acquisition; and (iv) the kinetic-energy dependence and the cluster-size dependence of the energy disposal.

Constant-energy MD simulations (using the fifth-order predictor–corrector method [6,9]) were performed for high-energy collisions of Kr_n ($n = 2$–512) clusters at center of mass velocities of $v = 5\times10^4$–10^7 cm s^{-1} (perpendicular to the surface) and initial center of mass kinetic energies $E_k^0 = 1$–10^6 eV, with a rigid Pt surface (Pt–Pt separation of 3.0 Å). The potential parameters between the Kr atoms and the Kr–Pt constituents were described by Lennard-Jones (LJ) potentials

$$u(r_{ij}) = 4\epsilon[(\sigma/r_{ij})^{12} - (\sigma/r_{ij})^6],$$

with $\sigma_{Kr,Kr} = 3.60$ Å, $\epsilon_{Kr,Kr} = 0.0147$ eV [33], $\sigma_{Kr,Pt} = 2.00$ Å and $\epsilon_{Kr,Pt} = 0.272$ eV [34]. The LJ potential at short distances overestimates the repulsive interaction, e.g., by a numerical factor of ≈ 2 for $u(r_{ij} = 1.98\ \text{Å}) = 100$ eV [35]. The isolated Kr_n clusters, prior to collision, were equilibrated at 10 K by heat pumping and subsequently the high-energy cluster–surface collision was simulated. The integration time step was $\Delta t \sim 10^{-15}$–10^{-17} s. For each simulation 20–100 trajectories were calculated with the equilibrated cluster initially oriented at random Euler angles with respect to the surface. The initial distance between the center of mass of the cluster and the surface was 20 Å, for which the cluster–wall interactions are negligible.

The high-energy cluster–surface collision (fig. 1) can be roughly separated into the following sequence of events: (i) the first stage involves the formation

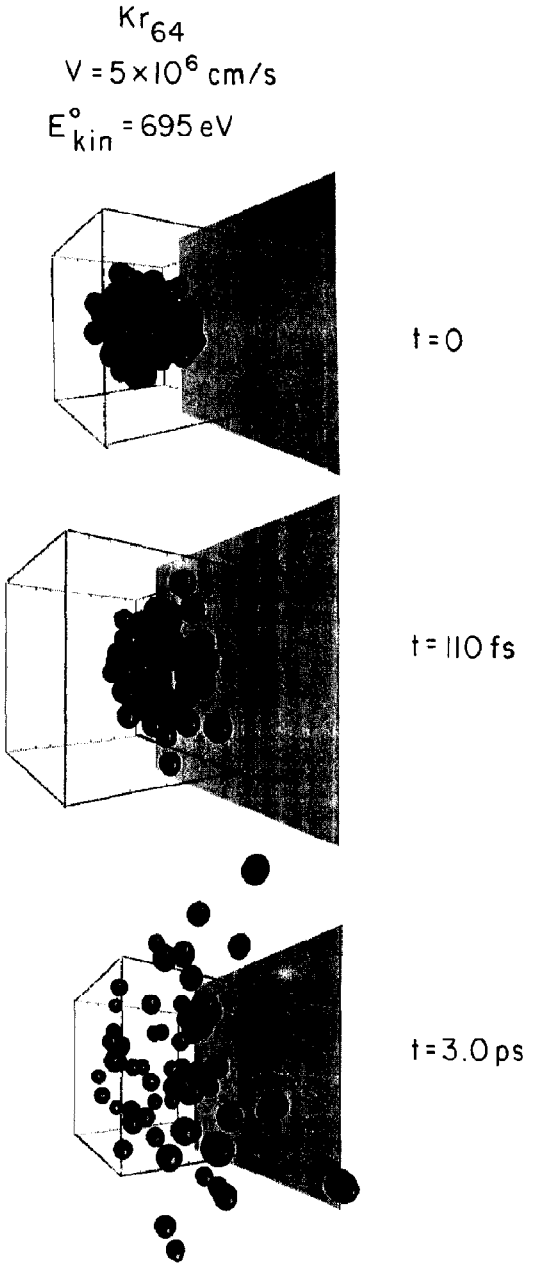

Fig. 1. Steps in the collision of a Kr_{64} cluster with a rigid Pt wall. At $t = 0$ (top picture) the cluster ($T = 10$ K) with initial velocity of 5×10^6 cm s^{-1} ($E_k^0 = 695$ eV) is located at a center of mass distance of 20 Å from the wall. At $t = 110$ fs (middle picture) the cluster collides with the wall, achieving its peak potential energy. At $t = 3.0$ ps (lower picture) cluster fragmentation occurred.

of a high surface density region of the outside cluster atomic layers which press into the surface; (ii) the second stage involves the reflection of the atoms of the middle part from the high-density surface region; and (iii) the third stage involves the formation of a collisional spike in the compressed cluster (middle picture in fig. 1) due to collisions between incoming and reflected layers. During the ultrashort collision time the energy is not equilibrated, but rather transferred from one atomic layer to another. Concurrently, extreme temperatures (obtained from the cluster kinetic energy corrected to the center of mass motion) of up to 3×10^5 K are generated during short collision times (10–10^2 fs) for $v=10^6$ cm s^{-1}. In view of the rigid surface description these temperatures are somewhat overestimated. This simulation provides a microscopic description of a cluster shock wave in a molecular cluster, in accord with model calculations for molecular droplets [20] and simulations for metal clusters [22,24].

A quantification of the energy acquisition process is obtained from the temporal evolution of the total potential energy, the cluster potential energy and the cluster–surface potential energy (fig. 2), which reveals that:

(1) Over the entire kinetic energy domain employed herein ($E_k^0/n\gtrsim0.5$ eV/particle) the cluster potential energy asymptotically approaches zero at long times, exhibiting cluster fragmentation to its atomic constituents, in accord with previous simulations [15,16]. The threshold kinetic energy (per particle) for complete cluster fragmentation is η^{-1} (ICPE/n), where ICPE is the isolated cluster potential energy (e.g. 9.1×10^{-2} eV for $n=64$) and η is the yield of kinetic energy disposition. Accordingly, $\eta\approx0.2$, indicating high energy conversion efficiency. This picture provides a microscopic analogue of meteorite–planet collisions [36].

(2) For moderately low kinetic energies, the negative asymptotic long-time cluster–surface potential energy reflects the adsorption of some atoms on the surface. With increasing E_k^0 the fragment absorption is diminished disappearing at $E_k^0/n>40$ eV.

(3) Stage (i) of the high-energy cluster–surface collision is manifested by a minimum in the cluster–surface potential energy, which is prominent at moderate E_k^0, while at higher E_k^0 the cluster is strongly

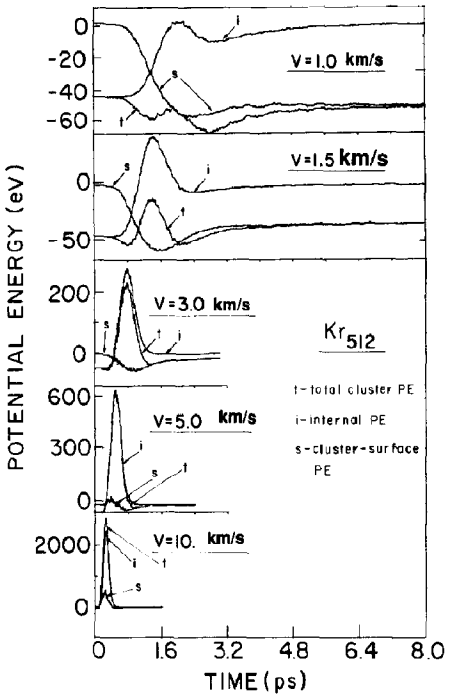

Fig. 2. Time evolution of the potential energy of a Kr_{512} cluster colliding with a Pt surface at various initial velocities (marked on the figure). t – the total cluster potential energy, i – the internal cluster potential energy and s – the cluster–surface potential energy.

pushed towards the surface revealing the repulsive cluster–surface potential energy.

(4) Stages (ii) and (iii) of the high-energy cluster–surface collisions are manifested by the maximum in the CPE.

(5) The total potential energy reveals the sequence of events (i) (point (3)) and (ii)+(iii) (point (4)). For $E_k^0\gtrsim300$–500 eV (e.g., $E_k^0/n\gtrsim1$ eV for $n=512$ and $E_k^0/n\gtrsim4$ eV for $n=64$) the prominent feature of the total potential energy is a peak reflecting the formation of a cluster shock wave (events (i)+(ii)+(iii)).

(6) A quantification of the time scale for the energy acquisition induced by the high-energy cluster–surface collision is provided by the cluster residence time τ, which was taken as the width of the prominent peak in the TPE. τ spans the range 20–500 fs (fig. 2), obeying the simple relation [20] $\tau\approx R/v$, with $R=14$ Å for $n=512$ and $R=7$ Å for $n=64$ (fig. 3). Thus $R\propto n^{-1/3}$, scaling as the cluster radius.

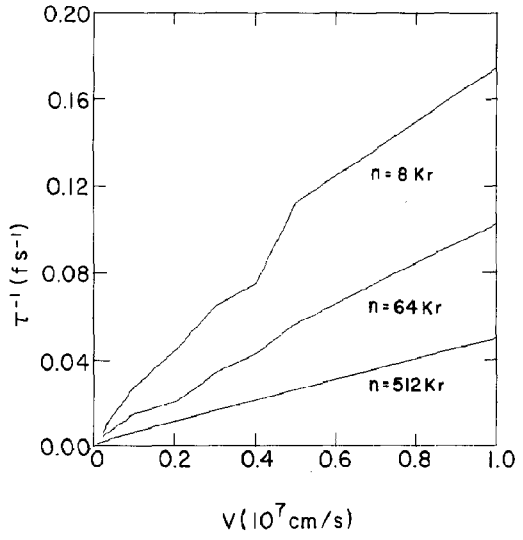

Fig. 3. The dependence of the inverse residence time of Kr_n ($n=8$, 64 and 512) clusters on the initial cluster velocity.

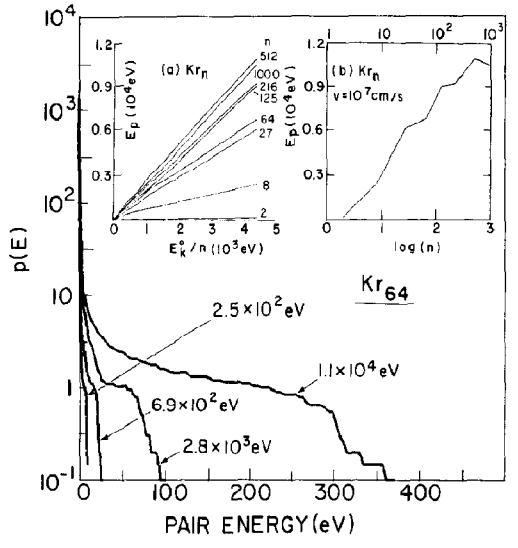

Fig. 4. The integral pair potential energy distribution $p(E)$ for a Kr_{64} cluster colliding with a Pt surface at various initial velocities ($v=3\times10^5$, 5×10^5, 10^6, 2×10^6 cm s^{-1}) with initial kinetic energies E_k^0 marked on the curves. The data were collected over 100 trajectories. Insert (a) (on the left side): The initial kinetic energy (per particle) dependence of the maximum single pair energy (E_p) in Kr_n ($n=2$–1000) clusters at the pinnacle of the HECSC (when the TPE assumes its highest value). Insert (b) (on the right side): The cluster-size dependence of E_p at $v=10^7$ cm s^{-1} ($E_k^0/n=4.3\times10^3$ eV).

A significant part of the cluster initial kinetic energy E_k^0 is converted into the cluster internal potential energy (fig. 4). The conversion efficiency of the cluster kinetic energy to the maximum value of the potential energy of interaction is 10%–20% for $n=8$–512. This high-yield atom energy is almost solely due to a single Kr–Kr pair repulsive interaction. The integral potential energy pair distributions (fig. 4) $p(E)=\int_E^\infty dE' N(E')$, where $N(E')$ is the differential pair potential energy distribution, clearly reveal high-energy tails. This behavior manifests the high-energy acquisition per single pair, which will allow the realization of pair energies in the range 10–10^4 eV (fig. 4a). The highest single pair energy E_p (fig. 4a) assumes large values up to $E_p\sim10^4$ eV. The pair energy accumulation factor $\alpha=E_p/(E_k^0/n)$ is close to unity, varying from $\alpha\approx0.6$ for $n=8$ to $\alpha\approx2.0$ for $n=512$. The pair energy yield $Y=E_p/E_k^0=\alpha/n$, varies in the range 10%–0.5%, decreasing with increasing n. The size dependence of E_p (at constant E_k^0/n) in the range $n=8$–512 obeys the scaling relation $E_p\propto n^\beta$ with $\beta\approx\frac{1}{3}$ (fig. 4b), i.e. $E_p\propto R$.

High-energy cluster–surface collisions result in a high-yield high-energy atomic pair interaction, which will induce outer-shell electronic excitations and ionization, multiple ionization and inner-shell Auger excitations of the atomic constituents. In rare-gas clusters outer-shell electronic excitations and ionization will be associative, e.g., $Kr+Kr\rightarrow Kr_2^*$ and $Kr+Kr\rightarrow Kr_2^+$, occurring at the intersection of the nuclear potential surfaces and their repulsive parts, which occur at pair energies close to the atomic electronic excitation and ionization, respectively. The cross section for such electronic processes can be approximated by the Landau–Zener formula [37] $\sigma\approx\pi r_1^2[1-\exp(-r_1/Vt)]$, where r_1 is the intersection distance of the potential curves, V the relative atomic velocity, while t is roughly the excited state lifetime, e.g., radiative lifetime $t\sim10^{-8}$ s or autoionization lifetime $t\sim10^{-15}$ s. At low velocities when $r_1/Vt\gg1$, $\sigma\approx\pi r_1^2$, while when $r_1/Vt\ll1$, $\sigma\approx\pi r_1^3/Vt$ and the cross section is low. The low-velocity limit will be accomplished when the pair energy will somewhat exceed the electronic excitation or ionization energy. Thus by a proper choice of E_k^0 (fig. 4), efficient electronic processes can be accomplished. Some experimental indication of electronic

excitation due to cluster collisions with a metal surface was reported [38].

From the point of view of chemical dynamics the high-energy cluster–surface collision provides a novel high-energy ultrashort energy acquisition process. The high internal energies and the energy acquisition times ($\tau = 10$–500 fs) for the "confined" cluster can be controlled by the initial cluster kinetic energy. These unique characteristics are chemically relevant for the induction of high-energy associative recombination and dissociation processes in atomic and small-molecule systems [38]. For large molecules the τ values span the time scale from vibrational frequencies to intramolecular vibrational relaxation times, opening up avenues for the exploration of intramolecular dynamics and isomerizations under extreme temporal and energetic conditions.

This research was supported by the German–Israel Binational James Franck Program for Laser–Matter Interactions and by a grant from the Commission for Basic Research administered by the Israel Academy of Sciences and Humanities (to UE).

References

[1] J. Jortner, Ber. Bunsenges. Physik. Chem. 88 (1984) 188.
[2] S. Bjørnholm, Contemp. Phys. 31 (1990) 309.
[3] J. Jortner, D. Scharf, U. Landman, N. Ben-Horin and U. Even, in: The chemical physics of atomic and molecular clusters (Proceedings of the International School of Physics "Enrico Fermi", Course CVII, 28 June–7 July 1988), ed. G. Scoles (North-Holland, Amsterdam 1990) p. 43.
[4] J. Jortner, Cluster size effects, Z. Physik D, in press.
[5] F. Amar and B.J. Berne, J. Phys. Chem. 88 (1984) 6720.
[6] D. Scharf, U. Landman and J. Jortner, J. Chem. Phys. 88 (1988) 4273.
[7] J.W. Bradey, J.D. Doll and D.L. Thompson, J. Chem. Phys. 73 (1980) 2767.
[8] J. Rose and R.S. Berry, J. Chem. Phys. 96 (1992) 517.
[9] A. Heidenreich, J. Jortner and I. Oref, J. Chem. Phys. 97 (1992) 197.
[10] E.E.B. Campbell, A. Tittes, D. Kranz, R. Schneider and A. Heilscher, Chem. Phys. Letters 184 (1991) 404.
[11] R. Schmidt, G. Seiferrt and H.O. Lutz, Phys. Letters A 158 (1991) 231, 237.
[12] J. Jellinek and Z.B. Guvenc, in: Nuclear Physics, Concepts in Atomic Cluster Physics, eds. H.O. Lutz, R. Schmidt and R. Dreizler (Springer, Berlin, 1992), in press.
[13] H.P. Kaukonen, U. Landman and C.L. Cleveland, J. Chem. Phys. 95 (1991) 4997.
[14] J. Gspann and G. Kreig, J. Chem. Phys. 61 (1974) 4037.
[15] G.Q. Xu, S.J. Bernasek and J.C. Tully, J. Chem. Phys. 88 (1988) 3376.
[16] G.Q. Xu, R.J. Holland, S.L. Bernasek and J.C. Tully, J. Chem. Phys. 90 (1989) 3831.
[17] H. Dietzel, G. Neukum and P. Rauser, J. Geophys. Res. 77 (1972) 1375.
[18] D. Smith and N.G. Adams, J. Phys. Appl. Phys. 6 (1973) 700.
[19] R.J. Beuhler and L. Friedman, Intern. J. Mass. Spectrom. Ion Phys. 23 (1977) 81.
[20] L. Friedman and G.H. Vineyard, Comments At. Mol. Phys. 15 (1984) 251.
[21] R. Beuhler and L. Friedman, Chem. Rev. 86 (1986) 521.
[22] M.H. Shapiro and T.A. Tombrello, Phys. Rev. Letters 65 (1990) 92.
[23] M.H. Shapiro and T.A. Tombrello, Phys. Rev. Letters 68 (1992) 1613.
[24] Y. Yamamura, Nucl. Instr. Methods Phys. Res. B 45 (1990) 707.
[25] J.F. Mahoney, J. Perel, T.D. Lee, P.A. Martino and P. Williams, J. Am. Soc. Mass Spectrom. 3 (1992) 311.
[26] E.R. Harrison, Phys. Rev. Letters 11 (1963) 535.
[27] R.J. Beuhler, G. Friedlander and L. Friedman, Phys. Rev. Letters 63 (1989) 1292.
[28] R.J. Beuhler, Y.Y. Chu, G. Friedlander, L. Friedman and W. Kunnmann, J. Phys. Chem. 94 (1990) 7665.
[29] C. Carraro, B.Q. Chen, S. Schramm and S.E. Koonin, Phys. Rev. A 42 (1990) 1379.
[30] S. Valkelathi, M. Manninen and E. Hammaren, Z. Physik D 22 (1992) 547.
[31] D.H. Lo, R.D. Pettrasso and K.W. Wenzel, Phys. Rev. Letters 68 (1992) 2107.
[32] R.J. Beuhler, G. Friedlander and L. Friedman, Phys. Rev. Letters 68 (1992) 2108.
[33] J.A. Barker, in: Rare gas solids, eds. M.L. Klein and N. Venables (Academic Press, New York, 1976) p. 212.
[34] G. Vidali, G. Ihm, H.-Y. Kim and M.W. Cole, Surface Sci. Rept. 12 (1990) No. 4.
[35] J.P. Biersack and J.F. Ziegler, Nucl. Instr. Methods 194 (1982) 93;
M.S. Daw and M.I. Baskes, Phys. Rev. B 29 (1984) 6443;
J.D. da Silva, J. Brandao and A.J.C. Varandas, J. Chem. Soc. Faraday Trans. 285 (1989) 1851.
[36] Y.B. Zeldovich and Yu.P. Raizer, Physics of shock waves and high-temperature hydrodynamic phenomena, Vol. 1 (Academic Press, New York, 1966).
[37] N.F. Mott and H.S.W. Massey, The theory of atomic collisions (Oxford Univ. Press, Oxford, 1965) p. 673.
[38] U. Even, P. de Lange, H. Jonkman and J. Kommandeur, Phys. Rev. Letters 56 (1986) 965.